Molecular Pharmacology Fast Forward. Published on September 23, 2005 as doi:10.1124/mol.105.012419
This article has not been copyedited and formatted. The final version may differ from this version.

MOL #12419

Nicotine Acts as a Pharmacological Chaperone to Upregulate Human α4β2 AChRs

A. Kuryatov, J. Luo, J. Cooper, and J. Lindstrom

Primary Laboratory of Origin:

Department of Neuroscience, University of Pennsylvania Medical School,

Philadelphia, PA 19104-6074

Molecular Pharmacology Fast Forward. Published on September 23, 2005 as DOI: 10.1124/mol.105.012419
This article has not been copyedited and formatted. The final version may differ from this version.

RUNNING TITLE PAGE

Running Title: AChR Upregulation

Corresponding Author: Jon Lindstrom, Department of Neuroscience, University of Pennsylvania Medical School, 217 Stemmler Hall 36th & Hamilton Walk, Philadelphia, Pennsylvania 19104

Fax: (215) 573-2015. Email: jslkk@mail.med.upenn.edu

Number of text pages: 48

Number of tables: 2

Number of figures: 14

Number of references: 40

Words in abstract: 194

Words in introduction: 564

Words in discussion: 1481

ABBREVIATIONS: AChR, acetylcholine receptor; ADNFLE, autosomal dominant nocturnal frontal lobe epilepsy; DHβE, dihydro-β-erythroidine hydrobromide; DMEM, Dulbecco's modified Eagle's medium; DMPP, 1,1-dimethyl-4-phenylpiperazinium iodide; DSP, Dithiobis (succinimidyl propionate); ER endoplasmic reticulum; HEK, human embryonic kidney; mAb, monoclonal antibody; MCC, methylcarbamylcholine; PBS, phosphate-buffered saline; SDS, sodium dodecyl sulfate; Sulfo-NHS-LC biotin, Sulfosuccinimidyl-6-(biotinamido) hexanoate.

Molecular Pharmacology Fast Forward. Published on September 23, 2005 as DOI: 10.1124/mol.105.012419
This article has not been copyedited and formatted. The final version may differ from this version.

ABSTRACT

Human neuronal nicotinic AChR α4 subunits and an α4 mutant (S247Fα4) found in autosomal dominant nocturnal frontal lobe epilepsy (ADNFLE) were expressed along with β2 in permanently transfected tsA201 HEK cell lines. Their sensitivity to activation, desensitization, and upregulation by cholinergic ligands was investigated. Upregulation after 3-24 hours resulted primarily from an increase in assembly of AChRs from large pools of unassembled subunits, but upregulation also resulted from a five-fold increase in the lifetime of AChRs in the surface membrane. Upregulation does not require current flow through surface membrane AChRs, because upregulation occurs in the presence of the channel blocker mecamylamine and with the α4 mutant which prevents nearly all AChR function. Both membrane-permeable ligands like nicotine and much less permeable quaternary amine cholinergic ligands can acts as pharmacological chaperones within the endoplasmatic reticulum to promote assembly of AChRs. Agonists are more potent pharmacological chaperones than are antagonists, presumably because activated or desensitized conformations assemble more efficiency. Assembly intermediates are disrupted by solubilization in Triton-X-100, but chemical crosslinking stabilizes a putative assembly intermediate about the size of an α4β2α4β2 tetramer.

Molecular Pharmacology Fast Forward. Published on September 23, 2005 as DOI: 10.1124/mol.105.012419
This article has not been copyedited and formatted. The final version may differ from this version.

INTRODUCTION

The effects of nicotine are complex. Nicotine is an agonist which can also function as a time-averaged antagonist by desensitizing nicotinic AChRs (Collins and Marks, 1996; Olale et al., 1997; Meyer et al., 2001; Gentry et al., 2003). Nicotine also causes an increase in the amount of AChRs (Peng et al., 1994; Wang et al., 1998; Whiteaker et al., 1998; Cooper et al., 1999; Perry et al., 1999; Gentry and Lukas, 2002).

AChRs have five homologous subunits organized around a central cation channel (Fig. 1) (Lindstrom, 2000). Acetylcholine binding sites in heteromeric neuronal AChRs are formed at the interface between an α2, α3, α4, or α6 subunit and a β2 or β4 subunit. A fifth "accessory" subunit, which does not take part in an acetylcholine binding site, is typically β2, β4, α5, or β3 (Lindstrom, 2000), but an α4 subunit can also occupy this position (Fig. 1) (Nelson et al., 2003; Zhou et al., 2003).

α4β2 AChRs are the primary brain subtype with high affinity for nicotine (Flores et al., 1991; Lindstrom, 2000) and are essential for nicotine self administration (Tapper et al., 2004; Maskos et al., 2005). Human α4β2 AChRs in our transfected HEK cell line are present in two stoichiometries $(\alpha4)_2(\beta2)_3$ and $(\alpha4)_3(\beta2)_2$ (Nelson et al., 2003; Fig. 1). The $(\alpha4)_2(\beta2)_3$ stoichiometry is more sensitive to activation and upregulation by nicotine and desensitizes more slowly. Properties of each stoichiometry expressed individually in *Xenopus* oocytes have been characterized (Zhou et al., 2003).

When α4β2 (Peng et al., 1994; Gopalakrishnan et al., 1997; Pacheco et al., 2001; Nelson et al., 2003; Xiao and Kellar, 2004; Sallette et al., 2004; 2005) or α3β2 AChRs (Wang et al., 1998; Xiao and Kellar, 2004) are expressed in transfected cells, nicotine can cause a large

increase in the quantity of AChRs. Upregulation of α3β2 AChRs occurs to the level at which α3β4 AChRs are constitutively expressed (Wang et al., 1998; Sallette et al., 2004). Susceptibility to nicotine-induced upregulation of α3β2 and α4β2 AChRs is regulated by a β2 microdomain located just above the acetylcholine binding site (Sallette et al., 2004). Nicotine-induced upregulation of transfected α3β2 AChRs (Wang et al., 1998) and α4β2 AChRs (Sallette et al., 2005) results primarily from an increase in assembly of large pools of pre-existing subunits, but there is also an increase in the half-life of surface membrane AChRs (Peng et al., 1994; Wang et al., 1998).

Here we show that nicotine acts as a pharmacological chaperone on an intracellular assembly intermediate to cause upregulation by promoting assembly of α4β2 AChRs, primarily by inducing an active or desensitized conformation which assembles more efficiently. During the prolonged incubation necessary for upregulation, quaternary amine agonists enter the lumen of the ER where they can also bind to nascent AChR binding sites and trigger increased AChR assembly. Nicotine further contributes to upregulation by increasing the lifetime of surface AChRs. In the continued presence of the concentrations of nicotine required for upregulation as found in typical smokers' sera (Benowitz, 1996), virtually all of the AChRs are desensitized. However, after removing nicotine, most, but not all, of the increased numbers of surface AChRs are functional. The S247Fα4 mutation, which causes ADNFLE (Steinlein, 2004), exhibits use-dependent activation in *Xenopus* oocytes (Kuryatov et al., 1997; Figl et al., 1998), but is virtually without function when expressed in HEK tsA201 cells. The homozygous mutant might similarly lack function in ADNFLE neurons.

Molecular Pharmacology Fast Forward. Published on September 23, 2005 as DOI: 10.1124/mol.105.012419
This article has not been copyedited and formatted. The final version may differ from this version.

MATERIALS AND METHODS

Cloning and tissue culture. The cDNAs for human α4, S247Fα4 and β2 subunits were cloned in this laboratory and described previously (Wang et al., 1996; Kuryatov et al., 1997). The subcloning of cDNA for human β2 into the expression vector pRc/CMV (Invitrogen, Carlsbad, CA) was described in Wang et al. (1998). The cDNAs for human α4 and S247Fα4 were subcloned into the restriction sites XhoI and BamHI of the selective mammalian expression vector pcDNA3.1/Zeo(-) (Invitrogen, Carlsbad, CA), which carries the Zeocin™ resistance gene. To establish stable cell lines, equal amounts of plasmids encoding α4 and β2 subunits were transfected into HEK tsA201 cells using the FuGene6 transfection agent (Roche Diagnostics, Indianapolis, IN) at a ratio of 5 μgDNA/15μl FuGene6 per 100 mm dish. Cloning rings were used to isolate individual clones. These were subsequently screened for highest stable expression using [^{3}H]epibatidine (DuPont NEN, Boston, MA) binding to live cells. Transfected cells were maintained in DMEM with penicillin (100 U/ml), streptomycin (100 μg/ml) (Invitrogen, Carlsbad, CA), and 10% fetal bovine serum (Hyclone, Logan, UT) as described previously (Wang et al., 1998). Zeocin (0.5 mg/ml; Invitrogen, Carlsbad, CA) was used for selection of α4, and G-418 (0.6 mg/ml; Invitrogen, Carlsbad, CA) was used for selection of β2 subunit expression.

Monoclonal antibodies (mAbs) used and solid phase radioimmunoassay. The rat IgG mAb 299 to α4 subunits, mAb 210 to the main immunogenic region on human α1, α3, α5, and β3 subunits, and mAb 295 to β2 subunits have been described previously (Lindstrom, 2000). These mAbs bind to the extracellular surface. mAb 295 binds strongly to β2 subunits when they

are assembled with α3, α4, or α6 subunits (Wang et al., 1998; Kuryatov et al., 1997; 2000) but not when they are expressed alone in HEK cells (Ren et al., 2005). The mouse IgG mAb 371 was raised to bacterially-expressed human AChR α4 subunits as described subsequently. It binds to the cytoplasmic surface of the α4 subunit.

Immulon 4 (Dynatech, Chantilly, VA) microtiter wells were coated with mAbs as previously described (Conroy et al., 1990). The cells were detached from plates by ice cold PBS (100 mM NaCl, 10 mM Na phosphate pH 7.4) with 5 mM EDTA and homogenized by repetitive pipetting in buffer A containing (in mM) 50 Na_2HPO_4-NaH_2PO_4, pH 7.5, 50 NaCl, 5 EDTA, 5 EGTA, 5 benzamidine, 15 iodoacetamide, and 2 phenylmethylsulfonyl fluoride. The membrane fractions were collected by centrifugation (20 min at 13,000 g). AChRs were solubilized by incubating the membrane fractions in buffer A containing 2% Triton X-100 at 25^{o}C for 1 hr. Insoluble material was removed by centrifugation for 20 min at 13,000 g. Solubilized AChRs from cells were used directly for all assays. mAb coated microtiter wells were incubated with Triton-solubilized AChRs and 2 nM [^{3}H]epibatidine at 25^{o}C for 3 hr. Then the wells were washed three times with PBS and 0.05% Tween-20 buffer before elution with 0.1M NaOH and transfer to Eppendorf tubes. The amount of bound radioactivity was determined using a 1450 Trilux Microbeta liquid scintillation counter (Wallac, Turku, Finland) with OptiPhase "Supermix" (Wallac, Turku, Finland). Nonspecific binding determined by incubation of extracts in parallel with 100 μM nicotine was subtracted from total and was less than 1% of total.

Total protein concentration of solubilized AChRs was determined using a BCA Protein Assay kit (Pierce, Rockford, IL).

FLEXstation experiments. For functional assays we used a FLEXstationII (Molecular

Molecular Pharmacology Fast Forward. Published on September 23, 2005 as DOI: 10.1124/mol.105.012419
This article has not been copyedited and formatted. The final version may differ from this version.

Devices, Sunnyvale, CA) benchtop scanning fluorometer basically as described by Fitch et al., (2003). The cells were plated at 70,000 cells/well on poly-D-lysine coated blackwall/clear bottom 96 well plates (Becton Dickinson, Franklin Lakes, NJ) the day before the experiment. Membrane Potential (excitation wavelength 530 nm and emission 565 nm) and Calcium Plus Assay Kits (excitation wavelength 485 nm and emission 525 nm) (Molecular Devices, Sunnyvale, CA) were used according to manufacturer protocols. Serial dilutions of drugs were prepared in V-shaped 96 well plates (Fisher Scientific, Pittsburgh, PA) and added in separate wells at a rate of 80 µl/sec during recording. Each point on curves represents the average response of 4 wells. The Hill equation was fitted to the concentration-response relationship using a nonlinear least-squares error curve fit method (KaleidaGraph, Abelbeck Software): $I(x) = I_{max}[x^n/(x^n+EC_{50n})]$, where $I(x)$ is current measured at the agonist concentration x, I_{max} is the maximal current response at the saturating agonist concentration, EC_{50} is the agonist concentration required for the half-maximal response and n is the Hill coefficient.

Binding of [^{3}H]epibatidine to living and fixed cells. Binding to living cells attached to 35 mm plates was done in DMEM at 4^{o}C for only 15 min with 0.5 nM [^{3}H]epibatidine to minimize ongoing upregulation and penetration of quaternary amines inside the cells. To determine the internal pool of epibatidine binding sites, 10 mM of the quaternary amine carbamylcholine was added together with 0.5 nM [^{3}H]epibatidine to inhibit binding to cell surface AChRs. Nonspecific labeling (around 1% of total) was determined by incubation with 100 µM nicotine and subtracted from total binding. After incubation, the cells were detached using 1ml ice cold PBS with 5 mM EDTA and washed three times with 1ml ice cold PBS by centrifugation (5 min at 500 g) in Eppendorf tubes. The washed pellets were dissociated with 100

Molecular Pharmacology Fast Forward. Published on September 23, 2005 as DOI: 10.1124/mol.105.012419
This article has not been copyedited and formatted. The final version may differ from this version.

µl of 0.1M NaOH, and bound radioactivity was determined in the same tubes using the scintillation counter with 1 ml per tube of scintillation fluid.

Prior to fixation, cells were grown to confluence in 100 µl of the media described above in 96-well microtiter plates with clear bottoms (Corning Inc., Corning, NY). Cells were then fixed with 100 µl of 4% phosphate buffered formaldehyde (Fisher Scientific, Fair Lawn, New Jersey) per well added for 1 hour at room temperature. After fixation, the cells were washed three times with 200 µl of PBS. Then 2.0 nM [^{3}H]epibatidine was added in 100 µl of PBS for 2 hours at room temperature. Assays were done in quadruplicate. Nonspecific binding was determined with the addition of 1 mM nicotine. Inhibition experiments were performed under the same conditions with added antagonists. To completely permeabilize fixed cells, they were treated for 1 hour with 100 µl of 0.1% Triton X-100 in PBS, then washed three times with 200 µl of PBS prior to labeling with epibatidine or iodinated mAbs. After labeling with [^{3}H]epibatidine, the wells were washed three times with 200 µl of PBS, and then 25 µl of 0.1M NaOH were added to elute [^{3}H]epibatidine. Bound radioactivity was determined in the same wells using 200 µl scintillation fluid per well. Fixation in 2% formaldehyde under these conditions results in the same amount of [^{3}H]epibatidine binding observed when labeling live cells for 30 minutes with 0.5nM [^{3}H]epibatidine (91±17%) and a similar K_D for epibatidine binding to membrane fractions (34±2 pM) and fixed cells (17±2 pM), but avoids the confounding problems of upregulation induced during labeling and prevents loss of cells during washing steps.

Upregulation in the presence of mecamylamine. The cells were plated on 24 well plates and grown until they reach 70 to 90% confluence. At this point 50 µM mecamylamine and

1 μM nicotine, 100 μM MCC, or 100 μM DMPP were added for 3hrs. After this incubation, the cells were fixed with equal volume of 4% phosphate buffered formaldehyde (Fisher Scientific, Fair Lawn, New Jersey) then washed three times with 1 ml of PBS before being incubated with 2 nM [^{3}H]epibatidine for 30min. After this incubation, the cells were washed three times with 1 ml of PBS before radioactive material was eluted by 200 μl of 0.1 M NaOH. Bound radioactivity was determined in Eppendorf tubes using 1 ml of scintillation fluid per tube. Protein concentrations were determined in a parallel experiment.

Upregulation of epibatidine binding sites in transfected cells. Cells were plated at a density of 50,000 cells per well in 96 well plates. The next day, when the cells were nearly confluent, ligands were added. The cells were incubated for another day and fixed as above by adding 100 μl of 4% phosphate buffered formaldehyde per well for 1 hour. All experiments were repeated at least twice. The data represent the average of all experiments.

DSP cross-linking. Cells were detached from a 10 cm dish using 10 ml of ice cold PBS, centrifuged, then resuspended in 1 ml of PBS. Crosslinking used a 1 mM concentration of DSP (Pierce, Rockford, IL) in 1ml of PBS for 2 hours on ice. The reaction was stopped by adding 10 μl of 1M Tris pH 7.5 for 15 min, then washing 3 times with 1 ml of ice cold PBS.

Sucrose gradients. Linear 5-20% sucrose gradients in 11.4 ml of 0.5% Triton X-100, PBS, 10 mM NaN_3 were layered with 200 μl samples and sedimented for 16 hours at 40,000 rpm in a Beckman SW41 rotor. Samples contained extracts from two 10 cm dishes plus 1 μl aliquots of 2 mg/ml purified *Torpedo* electric organ AChR as an internal sedimentation standard. After centrifugation, 10-drop fractions were collected from the bottom. From each fraction, 20 μl were

removed for assay of *Torpedo* AChR on microwells coated with mAb 210 (to α1 subunits). After labeling for 3 hours at 4°C with 2 nM [^{125}I]-α bungarotoxin, then washing 3 times with 200 µl of PBS+0.5% Triton X-100, these microwells were assayed in a gamma counter. From each fraction, another 20 µl were placed in microwells coated with mAb 295 (to β2 subunits) along with 2 nM [^{3}H]epibatidine. After incubation at room temperature for 3 hours, the wells were washed and placed in scintillation fluid prior to measurement in a scintillation counter.

Biotinylation. Cells from a confluent 10 cm dish were detached by 10 ml of ice cold PBS containing 1.8 mM $CaCl_2$ and 7.2 mM KCl, then washed in 10 ml of this buffer. The resuspended cells were labeled by EZ-link™ Sulfo-NHS-LC biotin (Pierce, Rockford, Il) at 1 mg/ml according to the manufacturer's protocol. After labeling, the cells were plated on 35 mm dishes and incubated again, with or without nicotine. Alternatively, AChRs were immediately solubilized in buffer A with 2% Triton X-100 as above. Biotin labeled solubilized AChRs were detected after extraction by binding to streptavidin agarose beads (Molecular Probes, Eugene, OR) or streptavidin (Sigma, St. Louis, MO) coated microtiter wells along with 2 nM [^{3}H]epibatidine.

Polyacrylamide gel electrophoresis. AChRs were extracted with 200 µl of 2% Triton X-100 in PBS per 10 cm dish. Samples were separated on 8% polyacrylamide tris-glycine gels or pre-cast Novex 7% polyacrylamide tris-acetate gels (Invitrogen, Carlsbad, CA) for α4 subunits, and 10% polyacrylamide tris-glycine for β2 subunits.

Preparation of mAb 371. Female BALB/c mice, 3-4 weeks of age, were obtained from Charles River Laboratories, Wilmington, MA. Human α4 subunits lacking the transmembrane

domains were constructed in the pET-26b(+) vector (Novagen, Madison, WI) and expressed in bacteria. They were solubilized in 3% SDS and 100 mM dithiothreitol, then purified by gel exclusion chromatography using Ultrogel AcA 34 (LKB, Uppsala, Sweden) with 0.1% SDS in PBS buffer. Most of the SDS was removed by dialysis before the purified α4 was used to immunize mice.

Mice were immunized at 4 intradermal sites in the lower back, and then boosted at three-week intervals with 40 μg/50 μl per mouse of α4 subunit construct emulsified in equal volume of TiterMax adjuvant. One final boost consisted of a mixture of 1 μg per mouse of α4β2 AChRs expressed in HEK cells isolated on mAb 295 coated beads and 10 μg per mouse of the bacterially-expressed subunit construct in incomplete Freund's adjuvant. The titers were monitored by test bleeds against α4 subunit in an ELISA assay. Five days after a final boost with antigen, splenic lymphocytes (~ 10^8) were harvested from the mouse with the highest titer and fused with SP2/0 myeloma cells (1×10^8) using 50% polyethylene glycol (Kodak 1450) before culture in 24 96-well plates (Costar, Corning, NY). Initial screening was done by ELISA assay as follows: Culture supernate from each well was diluted fifty-fold in PBS and 100 μl were added to corresponding wells of 24 96-well Immulon 4HBX flat-bottom microtiter plates (Thermo Labsystems, Franklin, MA) coated with 5 μg/ml of the α4 subunit and incubated overnight at 4^0C. After three washes, bound antibodies were detected by incubation for 1 hr with a 1:2000 dilution of biotin-labeled $F(ab)_2$ fragment to mouse IgG(H+L) (Kirkegaard & Perry Laboratories, Gaithersburg, MD), and 1-hr incubation with peroxidase labeled streptavidin (Kirkegaard & Perry Laboratories, Gaithersburg, MD), and a final incubation with 100 μl/well of SureBlue

TMB microwell peroxidase substrate (Kirkegaard & Perry Laboratories). Every incubation was followed by three washes except the final one. 100 μl of 1 M phosphoric acid was added to each well to stop the reaction. The absorbance at a wavelength of 450 nm was monitored with a Titertek Multiskan MCC/340. To eliminate those mAbs which crossreacted with closely related subunits, crossreaction with α3 in a similar solid phase assay was tested. Then mAbs which could detect both denatured α4 subunits and native α4β2 AChRs were selected using [^{3}H]epibatidine-labeled native α4β2 AChRs in RIAs. Positive hybridomas were cloned by a limiting dilution method.

RESULTS

Differential Activation and Upregulation of Two AChR Stoichiometries. Our α4β2 AChR cell line expresses both an $(\alpha4)_2(\beta2)_3$ and an $(\alpha4)_3(\beta2)_2$ stoichiometry. The arrangements of subunits in these two stoichiometries are shown in Figure 1. Initially we demonstrated these using electrophysiological methods in combination with quantification of methionine labeled subunits (Nelson et al., 2003), and we further characterized properties of the two AChR stoichiometries expressed individually in *Xenopus* oocytes (Zhou et al., 2003). Similar responses characteristic of the two stoichiometries can be obtained using fluorescent indicators sensitive to membrane potential or Ca^{++} concentration using cells grown in 96 well plates assayed in a Molecular Devices FLEXstation as shown in Figure 2. These two component response curves have been observed in another HEK cell line transfected with human α4β2 AChRs (Vallejo et al., 2005) but not in SH-EP1 cells transfected with human α4β2 (Pacheco et al., 2001) or in HEK

Molecular Pharmacology Fast Forward. Published on September 23, 2005 as DOI: 10.1124/mol.105.012419
This article has not been copyedited and formatted. The final version may differ from this version.

cells expressing rat or mouse α4β2 AChRs (Fitch et al., 2003; Karadsheh et al., 2004). The EC_{50} value for activation of the $(\alpha4)_3(\beta2)_2$ stoichiometry by nicotine (2.7 μM) is close to values reported for another human cell line in HEK cells (1.6 μM, Buisson et al., 1996 and 4.0 μM Gopalakrishnan et al., 1997) and for human α4β2 expressed in SH-EP1 cells (2.4 μM, Pacheco et al., 2001).

Nicotine selectively upregulates the sensitive $(\alpha4)_2(\beta2)_3$ stoichiometry, confirming the results previously detected electrophysiologically (Nelson et al., 2003) (Fig. 3). This also explains the observation of Vallejo et al. (2005) that upregulation "alters the functional state" resulting in increased sensitivity to activation and decreased desensitization. Initially there is a two-component dose response curve for nicotine (EC_{50}=116 and 2700 nM for the two stoichiometries). After nicotine treatment only a single component of the nicotine response curve is resolved (EC_{50}= 345 nM) due to a greater increase in the amount of the sensitive $(\alpha4)_2(\beta2)_3$ stoichiometry. Differences in sensitivity to activation by acetylcholine of the two AChR stoichiometries are sufficient to resolve separate EC_{50} values both before and after upregulation (Table 1). However, the two stoichiometries appear to exhibit similar sensitivities to activation by both DMPP and cytisine so that two components cannot be resolved in the response curves (Table 1).

Equilibrium binding of [^{3}H]nicotine reveals only a single component, presumably corresponding to a single desensitized state common to both stoichiometries (K_D=2.7±0.2 nM for wild type α4β2 and 2.4±0.7 nM for S247Fα4β2). Similarly, only a single binding component is resolved for [^{3}H]epibatidine (K_D=0.0172±0.0018 nM for wild type and 0.0396±0.0041 for

Molecular Pharmacology Fast Forward. Published on September 23, 2005 as DOI: 10.1124/mol.105.012419
This article has not been copyedited and formatted. The final version may differ from this version.

S247Fα4β2). Our wild type α4β2 AChR cell line expresses 0.9 pmoles epibatidine binding sites per mg of Triton-X-100 extracted protein prior to upregulation and 7.1 pmoles/mg after maximum upregulation. For the S247Fα4β2 cell line these values are 2.1 and 6.3 pmoles/mg.

Blocking AChR Function. The function of α4β2 AChRs can be blocked in several ways (Fig. 4). Mecamylamine noncompetitively blocks the cation channel (IC_{50}=770 nM). The competitive antagonist dihydro-β-erythroidine (DHβE) blocks acetylcholine binding (IC_{50}=88 nM). Nicotine, when added for a prolonged period, acts as a time-averaged antagonist by inducing a desensitized conformation. Nicotine is far more potent (IC_{50}=6 nM) than the other antagonists shown, and more potent as an antagonist than as an agonist (EC_{50}=120 nM and 2700 nM on the two stoichiometries) (Table 1). After 6 hours at the 200 nM nicotine concentration characteristic of cigarette smoker's serum (Benowitz, 1996), 90% of function is desensitized (Fig. 4).

Because nicotine-induced upregulation occurs over a matter of hours, the time averaged antagonist effect of nicotine in accumulating desensitized AChRs is probably more important for upregulation than its acute agonist effect. Comparison of the data in Figures 3 and 4 and Tables 1 and 2 make it clear that nicotine at its 35 nM EC_{50} for upregulation exceeds its 6 nm IC_{50} for antagonism, so that under the conditions used for upregulation virtually all the mature surface membrane AChRs are desensitized. Assembly intermediates which could bind nicotine, such an α4β2 dimers or α4β2α4β2 tetramers, are probably also similarly desensitized. The sensitivity to desensitization of such assembly intermediates might be less than that of mature AChRs in the cell surface. This could account for the difference between the EC_{50} for upregulation and the IC_{50}

for desensitization, if desensitization were a critical step in upregulation. The 35 nM EC_{50} for upregulation is below the 116 nM EC_{50} for activation of $(\alpha4)_2(\beta2)_3$ AChRs in the cell surface, and far below 2700 nM EC_{50} for activation of $(\alpha4)_3(\beta2)_2$ AChRs. Over the 6 hour exposure to nicotine in Figure 4, at concentrations which would produce no apparent acute activation of $(\alpha4)_3(\beta2)_2$ AChRs, all of the AChRs end up in a desensitized state. The long periods of incubation used in binding experiments with [^{3}H]nicotine or [^{3}H]epibatidine similarly convert all of the AChRs to the same desensitized state and reveal monotonic binding curves rather than the two component activation curves seen in Figures 2 and 3.

Upregulation Does Not Require Activation of Surface AChRs, Instead Membrane-Permeable Ligands Act Intracellularly as Molecular Chaperones. A HEK cell line transfected with the ADNFLE S247Fα4 mutation and β2 exhibits virtually no function by patch clamp recording (data not shown). No function could be detected with the mutant cell line by assay using membrane potential-sensitive fluorescent indicators under control conditions. After upregulation by nicotine a very small response was detectable, but the maximum was about 3% that of similarly upregulated wild type α4β2 AChRs (Fig. 5). Nonetheless, cholinergic ligands potently induce upregulation in the mutant cell (Fig. 5, Table 2).

Nicotine as well as the quaternary amines MCC and DMPP can induce upregulation of both wild type and S247Fα4β2 AChRs in the presence of 50 μM mecamylamine (Fig. 6), a concentration that blocks all current flow (Fig. 4). This further indicates that current flow is not required for upregulation. Upregulation of the amount of AChR is 3.3 fold more sensitive to the tertiary amine agonist nicotine and 7.6 fold to the tertiary agonist cytisine than is activation, but

it is 3.4 fold less sensitive to the quaternary amine agonist DMPP (Tables 1 and 2). That may correlate with the delay in penetration of quaternary amines inside the cells (see Fig. 9).

Upregulating AChR Function. The activity of α4β2 AChRs desensitized by nicotine can be recovered after removing the nicotine, resulting in a net gain in function due to upregulation during the period of agonist exposure (Fig. 7). The extent of upregulation in function is directly proportional to the increase in amount of AChRs on the cell surface (Fig. 8), thereby clearly revealing the mechanism by which increased assembly of AChRs results in increased function of AChRs.

This contrasts with the interpretation that nicotine causes an allosteric conformation change in pre-existing surface AChRs to account for the increased function observed (Vallejo et al., 2005). The slowing in desensitization and enhanced sensitivity observed after upregulation, which Vallejo et al. (2005) attribute to a conformation change of AChRs in the surface membrane, in fact reflect the increase in proportion of the $(\alpha4)_2(\beta2)_3$ stoichiometry after upregulation (Fig. 3; Nelson et al., 2003). The $(\alpha4)_2(\beta2)_3$ stoichiometry is more sensitive to nicotine and desensitizes less rapidly than the $(\alpha4)_3(\beta2)_2$ stoichiometry (Nelson et al., 2003; Zhou et al., 2003).

The extent of upregulation of function is less than the extent of upregulation of surface AChRs (i.e. the slope of the line in Fig. 8 is less than 1). This probably reflects irreversible desensitization of some of the AChRs (Gentry and Lukas, 2002; Gentry et al., 2003). An alternate explanation would be that nicotine, which had accumulated within the cells, partitioned out slowly, sustaining the AChRs in a reversibly desensitized state (Jia et al., 2003).

Molecular Pharmacology Fast Forward. Published on September 23, 2005 as DOI: 10.1124/mol.105.012419
This article has not been copyedited and formatted. The final version may differ from this version.

Acetylcholine Can Induce Upregulation. Incubation of cells with 300 μM acetylcholine does not induce upregulation (Fig. 9A), nor does a 10 μM concentration of the acetylcholinesterase inhibitor neostigmine. Added together so that acetylcholine remains intact, they cause upregulation equivalent to 1 μM nicotine (Fig. 9A). Acetylcholine upregulates both native α4β2 AChRs (Fig. 9A) and nonfunctional S247F α4β2 AChRs (data not shown). This indicates that the endogenous quaternary amine acetylcholine can increase the amount of AChRs by a mechanism that does not require function of the cation channel in AChRs on the cell surface.

Quaternary Amines Penetrate Inside Cells. Nicotine and epibatidine are tertiary amines which can readily cross cell membrane in their unprotonated form. In a 20 minute incubation both were very effective in inhibiting all specific binding of 5 nM [^{3}H]nicotine to AChRs in the α4β2 cell line (Fig. 9B). Quaternary amines would not be expected to cross cell membranes. After 20 minutes, a variety of quaternary amine agonists showed limited ability to inhibit binding of [^{3}H]nicotine to cells, as would be expected if they were binding only to surface AChRs (Fig. 9B). However, after 1 or 2 hours some of these ligands were able to inhibit virtually all specific binding. This surprising phenomenon has also been noted by others (Sallette et al., 2005; Vallejo et al., 2005). Thus, on prolonged incubation, quaternary amine agonists like ACh and TMA gain access to the interior of the ER and Golgi apparatus where they can bind to the acetylcholine binding sites of nascent AChRs. Darsow et al. (2005) attribute the upregulation produced by TMA to an effect on surface AChRs, but Fig. 9B shows that it can act on AChRs within the cell.

Molecular Pharmacology Fast Forward. Published on September 23, 2005 as DOI: 10.1124/mol.105.012419
This article has not been copyedited and formatted. The final version may differ from this version.

Agonists are More Potent at Upregulation than are Antagonists. A variety of nicotinic ligands can induce upregulation in these α4β2 AChR cell lines (Table 2). For example, the acetylcholine esterase antagonist and allosteric AChR affector galantamine (Samochocki et al., 2003), which is used to treat Alzheimer's disease, can also cause upregulation. The partial agonist cytisine equally potently upregulates α4β2 AChRs and the nonfunctional mutant. Even the competitive antagonist DHβE can cause upregulation. It is much less potent at upregulating (EC_{50}=32 μM) (Table 2) than antagonizing function (IC_{50}=0.088 μM) (Fig. 4, Table 1). The observation that agonists (nicotine, cytisine) are 3.3 to 7.6 fold more potent at upregulation than at activation of AChRs, while the antagonist DHβE is 364 fold less potent at upregulation than antagonizing activation of AChRs, suggests that the ability of agonists to induce the conformation changes associated with either activation or desensitization is important for potent upregulation by these ligands acting intracellularly as molecular chaperones. It has been suggested that upregulation is initiated by desensitization (Fenster et al., 1999). The maximum extent of activation which can be induced on wild type α4β2 AChRs by all agonists averages 5.3 fold, which is significantly greater than the maximum extent of upregulation by the antagonist DHβE (3.3 fold) or the allosteric affector galantamine (2.2 fold). This further suggests the importance of the ability to induce conformation changes associated with activation or desensitization in potency of upregulation. Similarly, 17-β-estradiol has been found to potentiate activation of α4β2 AChRs by binding to the C-terminus of α4 subunits (Paradiso et al., 2001), and we found that estrogen at 30 μM increases the extent of upregulation by nicotine ~25% during a 3 hour incubation (data not shown).

Molecular Pharmacology Fast Forward. Published on September 23, 2005 as DOI: 10.1124/mol.105.012419
This article has not been copyedited and formatted. The final version may differ from this version.

Nicotine induces upregulation much more potently (EC_{50}=35 nM) than it activates function (EC_{50}= 120 and 2700 nM for the two stoichiometries), but less potently than it binds at equilibrium to desensitized α4β2 AChRs (K_D = 2.8 nM). Similarly, epibatidine, a very high affinity agonist, induces upregulation less potently (EC_{50} = 3.6 nM) than it binds to desensitized α4β2 AChRs (K_D = 0.017 nM). These results suggest that agonists may induce upregulation by binding to AChR assembly intermediates with lower affinity than mature AChRs. Accurate comparisons are difficult, in part because the concentration of nicotine within the cells is not known. Nicotine crosses cell membranes very quickly (e.g. Fig. 9), and in some cells it can accumulate to much higher than ambient concentrations, e.g. in negatively charged compartments within *Xenopus* oocytes (Jia et al., 2003, and unpublished).

Increased Assembly of AChR Subunits Contributes to Upregulation. The time course of nicotine-induced upregulation revealed a rapid increase in mature α4β2 AChRs within the cells followed by an increase in surface AChRs after a lag of about 3 hours (Fig. 10A). The initial increase reflects rapid assembly of subunits from pre-existing pools in the ER. The pulse/chase labeling studies of Sallette et al. (2005) lead to this conclusion as well. The lag phase presumably reflects the time required for transport through the Golgi apparatus for modification of glycosylation before transport to the surface membrane. The accumulation of upregulated AChRs within the cells may indicate that processing of AChRs in the Golgi is a rate-limiting step.

Figs. 10B, C, and D use three different methods to demonstrate that upregulation by nicotine increases the proportion of total AChRs within the cell. Fig. 10B uses surface biotinylation with sulfo-NHS-LC biotin to label surface AChRs which are solubilized and

isolated with avidin prior to labeling with [^{3}H]epibatidine. This method may underestimate the absolute amount of AChRs on the cell surface if the biotinylation reagent does not label all surface AChRs, but it should accurately reflect changes in the amount of surface AChRs. Surface AChRs isolated on streptavidin coated wells were 35% of the total AChRs isolated on mAb 295 coated wells prior to upregulation. After upregulation, 25% were on the surface. Fig. 10C uses brief incubation with carbamylcholine to inhibit binding only to surface AChRs on live cells. By this assay 80% of the AChRs were on the surface prior to upregulation and 55% afterwards. These are probably reasonably accurate estimates. The tricky aspect of this assay is that carbamylcholine and epibatidine both induce upregulation, requiring that the total assay period is brief to minimize this effect. Fig. 10D uses binding of [^{125}I] mAb 295 plus or minus permeabilization on fixed cells. The subtleties of labeling with this mAb to β2 are discussed in the following paragraph. Prior to upregulation, mAb 295 labels a small amount of mature AChRs on the cell surface and a much larger amount of assembly intermediates within the cells. After upregulation, mAb 295 detects an increased proportion of mature AChRs on the cell surface and a consequently decreased proportion of assembly intermediates and fully assembled AChRs within the cells. All of these results are consistent with each other, Fig. 10A, Fig. 11 (to be subsequently discussed), and the pulse/chase labeling studies of Sallette et al. (2005) in proving that at short times upregulation results primarily from an increase in assembly of AChRs within the ER followed at later times by transport of the mature AChRs to the cell surface.

This contrasts with the hypothesis of Vallejo et al. (2005) who propose that nicotine induces a conformation change in pre-existing nonfunctional surface membrane AChRs which permits them to acquire high affinity binding of epibatidine and the ability to function in

response to agonist binding. They used the unusual approach for assaying surface membrane AChRs of employing the membrane permeable biotinylation reagent methanethiosulphonate ethylammonium biotin to label the cytoplasmic surface of surface membrane AChRs. They observed a fixed ratio of surface AChRs before and after upregulation, and on this basis argued that no new synthesis of AChRs was involved in upregulation. Their actual cholinergic ligand binding data for nicotine-induced upregulation is consistent with ours and that of Sallette et al. (2005), which is shown by several methods to result from increased assembly of mature AChRs within the cells.

The total amount [^{125}I] mAb 295 binding to permeabilized formalin fixed cells increases only 25% (from 5.6 to 7.3 fmoles/well) after upregulation with nicotine. This mAb to β2 subunits has the property that it does not bind with high affinity to β2 subunits expressed alone (Ren et al., 2005), but only binds to assembled α3β2, α4β2 or α6β2 AChRs (but not to α3β4, α4β4 or α6β4 AChRs) (data not shown). Thus, mAb 295 binds to an epitope on β2 whose conformation changes upon assembly with α subunits. The rat mAb 290 to β2 subunits has very similar properties (Sallette et al., 2005). The substantial amount of [^{125}I] mAb 295 binding to intact membranes prior to upregulation suggests that there is a large pool of assembly intermediates consisting of at least α4β2 pairs prior to upregulation. The association between α4 and β2 within assembly intermediates in intact membranes is easily disrupted by the detergent Triton X-100 as shown in Figs. 11 and 12. In Triton X-100 the subunits of mature AChR pentamers remain associated and the AChRs are efficiently solubilized. The assembly intermediates appear to have lower affinity for epibatidine than do mature AChRs. This would

Molecular Pharmacology Fast Forward. Published on September 23, 2005 as DOI: 10.1124/mol.105.012419
This article has not been copyedited and formatted. The final version may differ from this version.

account for higher affinity of [^{3}H]nicotine binding to mature immunoisolated α4β2 AChRs (K_D=2.7 nM) compared to the EC_{50} for upregulation of 35 nM and the K_D=0.017 nM for binding of [^{3}H]epibatidine compared to its EC_{50} for upregulation of 3.6 nM. This would also account for the ~5 fold increase in binding of [^{3}H]epibatidine after upregulation measured using 2 nM [^{3}H]epibatidine. The 25% increase in binding of [^{125}I] mAb 295 on upregulation would then reflect that prior to upregulation most α4 and β2 subunits are part of assembly precursors which exhibit the mature conformation of β2, moderate ligand binding affinity, and susceptibility to disruption by Triton X-100.

The total amount of binding of [^{125}I] mAb 371 to α4 subunits in the cells is the same before and after upregulation with 0.5μM nicotine for 20 hours. This indicates that the total pool of α4 subunits remains constant during upregulation. Unlike mAb 295, mAb 371 binds to both assembled native α4 subunits and to dissociated denatured subunits.

Large pools of dissociated α4 and β2 subunits are present in Triton X-100 extracts of this cell line (Fig. 11). Nicotine added overnight causes assembly of these subunits into mature AChRs. Nicotine causes no substantial increase in the total amount of subunits (i.e., it causes assembly of AChRs not synthesis of subunits).

Sucrose gradient sedimentation of Triton X-100 extracts showed that most epibatidine binding sites before and after upregulation by nicotine are concentrated at 10 S, as expected for pentameric α4β2 AChRs (Fig. 12A). The shoulder at 8.5 S on the peak of epibatidine binding may represent an assembly intermediate smaller than pentamers. The total amount of epibatidine binding sites in Triton X-100 extracts increased 13 to 20 fold (Fig. 12A) compared to a 3 to 5

fold increase of surface binding sites (Figs. 6 and 10) or a 5 fold increase in total epibatidine binding to fixed cells (Table 2). The greater extent of upregulation of epibatidine binding to mature AChRs in Triton extracts probably results because much of the epibatidine binding in cells prior to upregulation is to assembly intermediates of α4 and β2 subunits which are easily disrupted by Triton.

Western blots of sucrose gradient fractions revealed α4 subunits (Fig. 12B) and β2 subunits (data not shown) concentrated in the 10 S peak of mature AChR. There was no peak of unassembled subunits around 4-5 S where monomeric subunits would be expected. Instead, many unassembled subunits were observed at high apparent molecular weight (sedimenting faster than 10 S pentamers), suggesting that they were in association with large protein chaperones or were aggregated. mAb 295 to β2 subunits could not immunoprecipitate α4 subunits from fractions along gradients except in the case of 10 S mature AChRs, showing that in the presence of Triton X-100 any assembly intermediates between α4 and β2 were either dissociated or disrupted so that they were no longer recognizable by mAb 295 (data not shown).

Chemical Crosslinking May Stabilize the Labile Assembly Intermediate on Which Nicotine Acts as a Pharmacological Chaperone to Cause Upregulation. In order to try to stabilize an assembly intermediate of α4β2 AChRs which is disrupted by Triton X-100, and through which binding of nicotine in the ER might promote assembly of mature AChRs, α4β2 AChRs were treated with the crosslinking reagent DSP (Fig. 13). This revealed an epibatidine-binding 8.5 S component that could correspond to an assembly intermediate. This component would have to contain at least one α4β2 subunit pair in order to bind epibatidine (molecular

weight ≈119,000). This putative assembly intermediate is larger than 7 S IgG (molecular weight ≈150,000) and smaller than 9.5 S *Torpedo* AChR monomer (molecular weight ≈268,000), and thus could correspond to an α4β2α4β2 tetramer (molecular weight ≈239,000). Crosslinking inhibited some epibatidine binding and increased the sedimentation of mature AChRs somewhat, perhaps due to linkage to adjacent proteins or to changes in AChR conformation.

Increased AChR Half-Life Contributes to Upregulation. As in our human α3β2 AChR cell line (Wang et al., 1998) and chicken α4β2 AChR cell line (Peng et al., 1994), upregulation of α4β2 AChR depends not only on increased assembly of new AChRs, but also on an increase in the half-life of AChRs in the surface membrane (Fig. 14).

The increased lifetime of AChRs in nicotine apparently requires the continuous presence of nicotine. Gopalakrishnan et al. (1997) reported that if nicotine were removed after upregulation the number AChRs decreased with a $t_{1/2}$=11.7 hours. This is close to the $t_{1/2}$=12.6 hours which we measured for the loss of AChRs in cells which were never exposed to nicotine.

DISCUSSION

We propose that nicotine and other nicotinic ligands can act on an assembly precursor as pharmacological chaperones to cause upregulation by promoting assembly of mature AChR pentamers. In transfected cells there are large pools of subunits in the ER (Fig. 11, 12; Wang et al., 1998; Sallette et al., 2005). Many of these subunits are in assembly intermediates (Fig. 10D) about the size of α4β2α4β2 tetramers (Fig. 13; Sallette et al., 2004; 2005). The affinity of these assembly intermediates for nicotinic ligands is high, reflecting the potency of these ligands for

upregulating AChRs by this mechanism (Table 2), but probably lower than that for mature AChRs. For example, the EC_{50} for upregulation by nicotine is 35 nM while the K_D for binding to mature AChRs is 2.7 nM. The association of the subunits in assembly intermediates is easily disrupted by solubilization in Triton X-100 (Figs. 10-12) but can be stabilized to solubilization in Triton X-100 by crosslinking with DSP (Fig. 13). When nicotine binds to assembly intermediates, it acts as a pharmacological chaperone. Binding of ligands to the ACh binding site at the interface between α4 and β2 subunits may stabilize assembly intermediates, resulting in increased amounts of intermediates and consequently of mature AChRs. Binding of agonists may also promote conformation changes in the assembly intermediate corresponding to those the agonist would produce during activation or desensitization, and these conformation changes may further promote assembly of mature AChRs. This would account for the far greater potency of agonists than antagonists as pharmacological chaperones. If the assembly intermediates were α4β2α4β2 tetramers with two ACh binding sites, final assembly would consist only of addition of a β2 subunit in the accessory position. The precise pathway of α4β2 AChR assembly remains to be determined.

The agonist-mediated conformation changes in the acetylcholine binding protein described by Gao et al. (2005) reflect the sorts of interactions which may be involved in molecular chaperone effects. As acetylcholine enters the binding site it brings together conserved tryptophan residues from adjacent subunits. This might be a “molecular glue” effect shared by agonists and antagonists which would help to stabilize the association of α4 and β2 in assembly intermediates. Acetylcholine was found to cause a large movement of the C loop to close access

to the binding site and mediate new contacts between subunits across the binding site including hydrogen bonds between side chains on the loop and the opposing β8-β9 linker. This might reflect the agonist-induced conformation change through which nicotine and other agonists gain great potency in promoting the assembly of AChR subunits.

The surprising observation that after prolonged incubation quaternary amine cholinergic ligands gain access to the interior of the ER is also supported by the observations of others (Sallette et al., 2005; Vallejo et al., 2005). Thus, both rapidly membrane-permeable ligands like nicotine and very slowly membrane-permeable ligands like MCC can act as pharmacological chaperones.

The upregulated AChRs can function in the surface membrane (Figs. 3, 7 and 8) after recovering from desensitization or antagonism by the drug (Fig. 4). Human α4β2 AChRs in the presence of the 0.2 μM nicotine concentrations sustained in the sera of cigarette smokers (Benowitz, 1996) are substantially increased in amount over 6 hours (Figs. 8 and 10), but 90% are desensitized (Fig. 4) in the continued presence of this concentration of nicotine. By 1 hour after the washout of this concentration of nicotine, 82% of the AChRs present can be activated by nicotine (Fig. 8).

Studies of our human α4β2 AChR cell line have revealed a fundamental new insight into nicotine-induced upregulation: nicotine can act as a pharmacological chaperone to promote assembly of AChR subunits. This concept is also supported by the studies of Sallette et al., (2004; 2005). Pharmacological chaperones have previously been found to promote the conformational maturation of single subunit metabotropic receptors for opioids and vasopressin

Molecular Pharmacology Fast Forward. Published on September 23, 2005 as DOI: 10.1124/mol.105.012419
This article has not been copyedited and formatted. The final version may differ from this version.

(Morello et al., 2000; Petaja-Repo et al., 2002).

These studies conflict with the mechanism of nicotine-induced upregulation proposed by Vallejo et al. (2005). They propose that nicotine converts AChRs already in the surface membrane to a state which binds more epibatidine, is more sensitive to activation, and desensitizes more slowly. We show that the increase in epibatidine binding and increase in response to agonists at 3-24 hours is primarily due to assembly of new mature 10 S AChRs. The increased sensitivity to activation and reduced rate of desensitization results from the selective upregulation of the $(\alpha4)_2(\beta2)_3$ stoichiometry, which has these properties.

In addition to promoting the assembly of the new AChRs, nicotine also contributes to upregulation by increasing the half-life of AChRs in the surface membrane (Fig. 14; Peng et al., 1994; Wang et al., 1998). Increased half-life of surface AChR might be caused by a post-translational modification subsequent to desensitization. In the presence of nicotine virtually all AChRs are desensitized (Fig. 4). The five fold increase in half-life of human α4β2 AChRs caused by nicotine (Fig. 14) could contribute substantially to upregulation over several days. In transfected cells with large pools of unassembled subunits, large increases of AChRs within the cells can accumulate within 3 hours as a result of increased assembly, while smaller increases in surface AChRs become apparent after 5 hours (Fig. 10A). In neurons without large pools of unassembled subunits, upregulation due to reduced degradation of surface AChRs alone would be more than sufficient to explain the extent of nicotine-induced upregulation observed in brain (Perry et al., 1999).

The nicotine-induced increase in lifetime of surface membrane human AChRs which we describe here and the nicotine-induced increase in lifetime of chicken α4β2 AChRs (Peng et al.,

1994) and human α3β2 (Wang et al., 1998) has not been observed in other studies (Sallette et al., 2005; Vallejo et al., 2005; Darsow et al., 2005). All of our studies which detected a nicotine-induced increase in AChRs lifetime used permanently transfected lines. Sallette et al. (2005) transiently transfected HEK cells with human α4β2 AChRs, which may have inhibited detection of this effect measured in experiments over 50 hours in our permanently transfected cell line. Vallejo et al. (2005) permanently transfected a HEK cell line with rat α4β2 AChRs. Species-specific effects may be important in this case. Also, instead of biotinylating the extracellular surface of AChRs as we did to identify surface AChRs in turnover experiments, they used a reagent which biotinylated the cytoplasmic surface of the AChRs, and this might influence their results. Their biotinylation method also did not detect the initial nicotine-induced increase in newly assembled AChRs in the ER demonstrated by pulse-chase labeling by Sallette et al. (2005) or by three other methods in Figure 10. Darsow et al. (2005) using HEK cells transiently transfected with mouse α4β2 did not detect a nicotine-induced increase in lifetime. They agree that nicotine increased assembly, but detected only 1.8% of the amount of AChRs which we detect in our permanently transfected cell line. The very rapid rate of internalization of surface AChRs which they observe (60%/30 minutes) may be a species-specific effect which accounts for their low level of expression and lack of detection of an effect of nicotine on AChR lifetime.

The lack of function of S247Fα4 β2 AChRs (Fig. 5) does not prevent upregulation of AChRs by ligands acting as pharmacological chaperones. The ADNFLE mutation S247F in the channel lining M2 region of α4 subunits alters the function of α4β2 AChRs expressed in *Xenopus* oocytes (Kuryatov et al., 1997). This mutation virtually completely prevents function

Molecular Pharmacology Fast Forward. Published on September 23, 2005 as DOI: 10.1124/mol.105.012419
This article has not been copyedited and formatted. The final version may differ from this version.

when these AChRs are expressed in HEK cells (Fig. 5). Loss of function by this mutant in HEK cells may be in part because 80% of the AChRs in this cell line have an $(\alpha4)_3(\beta2)_2$ stoichiometry, whereas, at appropriate ratios of subunit mRNAs, virtually all of the AChRs expressed in oocytes can have an $(\alpha4)_2(\beta2)_3$ stoichiometry (Zhou et al., 2003). With the $(\alpha4)_3(\beta2)_2$ stoichiometry of the mutant, three phenyl groups in the M2 channel lining transmembrane domain are in the channel rather than two in the $(\alpha4)_2(\beta2)_3$ stoichiometry. The replacement of three serines in the channel by three phenyl groups may almost completely prevent current flow in the $(\alpha4)_3(\beta2)_2$ stoichiometry of the mutant. This idea is supported by the observation (data not shown) that transient transfection of the mutant line with either β3 or α5 subunits produces AChRs with abundant function. Addition of these accessory subunits would result in $(\alpha4)_2(\beta2)_2\alpha5$ or $(\alpha4)_2(\beta2)_2\beta3$ stoichiometries with only two phenyl groups in the channel. In *Xenopus* oocytes, S247Fα4β2 AChRs are only weakly activated by the first application of agonist, but subsequently they are efficiently activated (Kuryatov et al. 1997; Figl et al., 1998). These mutant AChRs desensitize faster than wild type, have reduced inward rectification, and virtually no Ca^{++} permeability. If S247F α4β2 AChRs were as inactive in ADNFLE neurons as in HEK cells, the effects of this mutation in the homozygous state would be greater than experiments in *Xenopus* oocytes have suggested.

ACKNOWLEDGEMENTS

We thank Drs. Gregg Wells, Rene Anand, and Barbara Campling for their comments in

the manuscript.

REFERENCES

Benowitz N (1996) Pharmacology of nicotine: addiction and therapeutics. *Ann Rev Pharmacol Toxicol*. **36**:597-613.

Buisson B, Gopalakrishnan M, Arneric SP, Sullivan JP, and Daniel D (1996) Human α4β2 neuronal nicotinic acetylcholine receptor in HEK 293 cells: a patch-clamp study. *J. Neurosci* **16**: 7880 – 7891.

Collins A and Marks M (1996) Are nicotinic receptors activated or inhibited following chronic nicotine treatment? *Drug Dev Res* **38**:231-242.

Conroy WG, Saedi MS and Lindstrom J (1990) TE671 cells express an abundance of a partially mature acetylcholine receptor α subunit which has characteristics of an assembly intermediate. *J Biol Chem* **265**:21,642-21,651.

Cooper S, Harkness P, Baker E and Millar N (1999) Upregulation of cell surface α4β2 neuronal nicotinic receptors by lower temperature and expression of chimeric subunits. *J Biol Chem* **274**:27,145-27,152.

Darsow T, Booker TK, Pina-Crespo JC and Heinemann SF (2005) Exocytic trafficking is required for nicotine-induced upregulation of α4β2 nicotinic acetylcholine receptors. *J Biol*

Chem **280**: 18311-18320.

Fenster CP, Beckman ML, Parker JC, Sheffield EB, Whitworth TL, Quick MW and Lester RA (1999) Regulation of α4β2 nicotinic receptor desensitization by calcium and protein kinase C. *Mol Pharmacol* **55**: 432-43.

Figl A, Viseshakul N, Shafaee N, Forsayeth J and Cohen BN (1998) Two mutations linked to nocturnal frontal lobe epilepsy cause use-dependent potentiation of the nicotinic ACh response. *J Phisiol (Lond)* **513**: 655-670.

Fitch RW, Xiao Y, Kellar KJ and Daly JW (2003) Membrane potential fluorescence: a rapid and highly sensitive assay for nicotinic receptor channel function. *Proc Natl Acad Sci USA* **100**:4909-4914.

Flores CM, Rogers SW, Pabreza LA, Wolfe BB and Kellar KJ (1992) A subtype of nicotinic cholinergic receptor in rat brain is composed of alpha 4 and beta 2 subunits and is upregulated by chronic nicotine treatment. *Mol Pharmacol* **41**:31-37.

Gao F, Bren N, Burghardt TP, Hansen S, Henchman RH, Taylor P, McCammon JA and Sine SM (2005) Agonist-mediated conformational changes in acetylcholine-binding protein revealed by simulation and intrinsic tryptophan fluorescence. *J Biol Chem* **280**:8,443- 8,451.

Gentry C and Lukas R (2002) Regulation of nicotinic acetylcholine receptor numbers and function by chronic nicotine exposure. *Curr Drug Target CNS Neurol Disord* **1**:359-385.

Gentry C, Wilkins L and Lukas R (2003) Effects of prolonged nicotinic ligand exposure on function of heterologously expressed human α4β2 and α4β4 nicotinic acetylcholine receptors. *J Pharm Exp Ther* **304**:206-216.

Gopalakrishnan M, Molinari EJ, and Sullivan JP (1997) Regulation of human α4β2 neuronal nicotinic acetylcholine receptors by cholinergic channel ligands and second messenger pathways. *Mol Phartmacol* **52**:524-534.

Jia L, Flotides K, Li M and Cohen B (2003) Nicotine trapping causes the persistent desensitization of α4β2 nicotinic receptors expressed in oocytes. *J Neurochem* **84**:753-766.

Karadsheh MS, Shah MS, Tang X, Macdonald RL and Stitzel JA (2004) Functional characterization of mouse α4β2 nicotinic acetylcholine receptors stably expressed in HEK293T cells. *J Neurochem* **98**:1138-1150.

Kuryatov A, Gerzanich V, Nelson M, Olale F and Lindstrom J (1997) Mutation causing autosomal dominant nocturnal frontal lobe epilepsy alters Ca^{++} permeability, conductance, and gating of human α4β2 nicotinic acetylcholine receptors. *J Neurosci* **17**:9035-9047.

Kuryatov A, Olale F, Cooper J, Choi C and Lindstrom J (2000) Human α6 AChR subtypes: subunit composition, assembly, and pharmacological responses. *Neuropharmacology* **39**:2570-2590.

Lindstrom JM (2000) The structure of neuronal nicotinic receptors, in *Neuronal Nicotinic Receptors* (Clementi F, Gotti C and Fornasari D eds) vol 144 pp 101-162, Springe-Verlag New York In., New York, Handbook of Experimental Pharmacology.

Maskos U, Molles BE, Pons S, Besson M, Guiard BP, Guilloux JP, Evrard A, Cazala P, Cormier A, Mameli-Engvall M, Dufour N, Cloez-Tayarani I, Bemelmans AP, Mallet J, Gardier AM, David V, Faure P, Granon S and Changeux JP (2005) Nicotine reinforcement and cognition restored by targeted expression of nicotinic receptors. *Nature* **436**:103-107.

Morello J-P, Salahpour A, Laperriere A, Vernier V, Arthus M-F, Lonergan M, Petaja-Repo U, Angers S, Marin D, Bichet D and Vouvier M (2000) Pharmacological chaperones rescue cell-surface expression and function of misfolded V2 vasopressin receptor mutants. *J Clin Investig* **105**:887-895.

Nelson ME, Kuryatov A, Choi CH, Zhou Y and Lindstrom JM (2003) Alternate stoichiometries of α4β2 nicotinic acetylcholine receptors. *Mol Pharmacol* **63**:332-341.

Olale F, Gerzanich V, Kuryatov A, Wang F and Lindstrom J (1997) Chronic nicotine exposure differentially affects the function of human α3, α4, and α7 neuronal nicotinic receptor subtypes. *J Pharm Exp Ther* **283**:675–683.

Pacheco MA, Pastoor TE, Lukas RJ and Wecker L (2001) Characterization of human α4β2 neuronal nicotinic receptors stably expressed in SH-EP1 cells. *Neurochem Res* **26**:683 – 693

Paradiso K, Zhang J and Steinbach JN (2001) The C Terminus of the human nicotinic α4β2 receptor forms a binding site required for potentiation by an estrogenic steroid. *J Neurosci* **21**:6561-6568.

Peng X, Anand R, Whiting P and Lindstrom J (1994) Nicotine-induced upregulation of neuronal nicotinic receptors results from a decrease in the rate of turnover. *Mol Pharmacol* **46**:523-530.

Perry D, Davila-Garcia M, Stockmeier C and Kellar K (1999) Increased nicotinic receptors in brains from smokers: membrane binding and autoradiography studies. *J Pharm Exp Ther* **289**:1545-1552.

Petaja-Repo V, Hogue M, Bhalla S, Laperriere A, Morello J-P and Voucier M (2002) Ligands act as pharmacological chaperones and increase the efficiency of δ opioid receptor maturation. *EMBO (Eur Mol Biol Organ) J*. **21**:1628-1637.

Ren X-Q, Cheng S-B, Treuil MW, Mukherjee J, Rao J, Braunewell KH, Lindstrom JM and Anand R (2005) Structural determinants of α4β2 nicotinic acetylcholine receptor trafficking. *J Neurosci* **25**:6676-6686.

Sallette J, Bohler S, Benoit P, Soudant M, Pons S, Novere N, Changeux J-P and Corringer P (2004) An extracellular protein microdomain controls upregulation of neuronal nicotinic acetylcholine receptors by nicotine. *J Biol Chem* **279**:18,767-18,775.

Sallette J, Pons S, Devillers-Thiery A, Soudant M, Carvalho LP, Changeux JP and Corringer PJ (2005) Nicotine upregulates its own receptors through enhanced intracellular maturation. *Neuron* **46**: 595-607.

Samochocki M, Hoffle A, Feherenbacher A, Jostoc R, Ludwig J, Christner C, Radia M, Zerlin M, Ulliner C, Pereira E, Lubbert H, Albuquerque E and Maelicke A (2003) Galantamine is an allosteric potentiating ligand of neuronal nicotinic but not muscarinic acetylcholine receptors. *J Pharm Exp Ther* **305**:1024-1036.

Steinlein O. (2004) Genetic mechanisms that underlie epilepsy. *Nature Rev Neurosci* **5**:400-408.

Tapper AR, McKinney SL, Nashmi R, Schwarz J, Deshpande P, Labarca C, Whiteaker P, Marks MJ, Collins AC, Lester HA (2004) Nicotine activation of α4* receptors: sufficient for reward,

tolerance, and sensitization. *Science* **306**:1029-1032.

Vallejo YF, Buisson B, Bertrand D and Green WN (2005) Chronic nicotine exposure upregulates nicotinic receptors by a novel mechanism. *J Neurosci* **25**: 5563-72.

Wang F, Gerzanich V, Wells GB, Anand R, Peng X, Keyser K and Lindstrom J (1996) Assembly of human neuronal nicotinic receptor α5 subunits with α3, β2 and β4 subunits. *J Biol Chem* **271**:17,656-17,665.

Wang F, Nelson M, Kuryatov A, Keyser K and Lindstrom J (1998) Chronic nicotine treatment upregulates human α3β2 but not α3β4 AChRs stably transfected in human embryonic kidney cells. *J Biol Chem* **273**:28,721-28,732.

Whiteaker P, Sharples C and Wonnacott S (1998) Agonist-induced upregulation of α4β2 nicotinic acetylcholine receptors in M10 cells: pharmacological and spatial definition. *Mol Pharmacol* **53**:950-962.

Xiao Y and Kellar KJ (2004) The comparative pharmacology and up-regulation of rat neuronal nicotinic receptor subtype binding sites stably expressed in transfected mammalian cells. *J Pharm Exp Ther*. **310**:98-107.

Zhou Y, Nelson M, Kuryatov A, Choi C, Cooper J and Lindstrom J (2003) Human α4β2 AChRs

formed from linked subunits. *J Neurosci* **23**:9004-9015.

Molecular Pharmacology Fast Forward. Published on September 23, 2005 as DOI: 10.1124/mol.105.012419
This article has not been copyedited and formatted. The final version may differ from this version.

FOOTNOTES

This work was supported by grants to Jon Lindstrom from the National Institute of Health (NS11323) and the Philip Morris External Research Program.

Corresponding Author: Jon Lindstrom, Department of Neuroscience, University of Pennsylvania Medical School, 217 Stemmler Hall 36th & Hamilton Walk, Philadelphia, Pennsylvania 19104. E-mail: jslkk@mail.med.upenn.edu

Molecular Pharmacology Fast Forward. Published on September 23, 2005 as DOI: 10.1124/mol.105.012419
This article has not been copyedited and formatted. The final version may differ from this version.

LEGENDS FOR FIGURES

Fig. 1. Comparison of the putative subunit arrangements in alternate α4β2 AChR stoichiometries with the subunit arrangement in *Torpedo* AChR.

Fig. 2. Activation by acetylcholine of α4β2 AChRs expressed in the HEK cell line assayed in microwell plates using the FLEXstation and its proprietary fluorescent indicators reveals activity of both the sensitive $(\alpha4)_2(\beta2)_3$ stoichiometry and the insensitive $(\alpha4)_3(\beta2)_2$ stoichiometry. The higher proportion of response detected in the Ca^{++} sensitive indicator reflects the higher Ca^{++} permeability of the $(\alpha4)_3(\beta2)_2$ stoichiometry (data not shown). Responses were normalized to the maximum response.

Fig. 3. Nicotine selectively upregulates the sensitive $(\alpha4)_2(\beta2)_3$ stoichiometry in the α4β2 AChR cell line. AChR function was assayed using the FLEXstation. Both an $(\alpha4)_2(\beta2)_3$ and an $(\alpha4)_3(\beta2)_2$ stoichiometry are clearly present in control cells. The more sensitive $(\alpha4)_2(\beta2)_3$ stoichiometry predominates after nicotine treatment. Responses were normalized to the maximum α4β2 AChR response after treatment with nicotine. A membrane potential-sensitive indicator was used.

Fig. 4. α4β2 AChR function can be blocked by competitive and noncompetitive antagonists, and even more potently by nicotine which desensitizes the AChRs. Antagonists were added 30

minutes before assay. Nicotine was added for 6 hours prior to assay. Responses to 3 μM acetylcholine were determined. -○- Antagonism by the non-competitive channel blocker mecamylamine, IC_{50}=770 nM. -□- Antagonism by the competitive acetylcholine binding site blocker DHβE, IC_{50}=88 nM. -▲- The time averaged antagonist effect of desensitization by nicotine, IC_{50}=6.1 nM. Responses were normalized to control responses without antagonist. A membrane potential sensitive indicator was used.

Fig. 5. The S247Fα4β2 line exhibits virtually no AChR function, but nicotine upregulates the amount of AChRs to the same extent as wild-type α4β2 AChRs. Function was assayed after upregulation overnight with 0.5 μM nicotine followed by a wash for 1 hour to permit detection of the tiny response of the S247Fα4β2 AChRs. A membrane potential sensitive indicator was used to assay function. Responses were normalized to the maximum wild-type α4β2 AChR response.

Fig. 6. The channel blocker mecamylamine does not block upregulation. Mecamylamine was used at 65 fold its IC_{50} for noncompetitively blocking function. The amount of AChR after 3 hours upregulation was measured by [^{3}H]epibatidine binding to fixed cells. Both the tertiary amine nicotine and the quaternary amines MCC and DMPP were used in both wild-type α4β2 AChRs expressing cells (A) and nonfunctional S247Fα4β2 AChRs cells (B). Failure of channel block to prevent upregulation and the ability of nonfunctional AChRs to efficiently upregulate proves that upregulation is not triggered by current flow through AChRs in the surface

membrane.

Fig. 7. Nicotine treatment increases the number of functional AChRs detectable after a 1 hour wash to reverse the desensitizing effects of nicotine. The responses to various concentrations of nicotine are shown A) in the absence and B) in the presence of treatment overnight with 0.5 μM nicotine. A membrane potential sensitive indicator was used**.**

Fig. 8. Overnight exposure to nicotine increases surface α4β2 AChRs in direct proportion to the increase in AChR function (assayed after a 1 hour wash). The slope of the line is less than 1. The decrement reflects the fraction of AChRs which are irreversibly desensitized under these conditions. The number over each point in the graph is the nicotine concentration used for overnight incubation. Surface upregulation was determined as the difference between total binding of 0.5nM [^{3}H]epibatidine for 15 minutes and its binding in the presence of 10 mM carbamylcholine to block epibatidine binding to surface AChRs. Thus, at 50 nM nicotine, the amount of AChRs on the surface increases 3.3 fold, but the response to acetylcholine increases only 2.3 fold.

Fig. 9. Quaternary amines can penetrate inside cells and induce upregulation. A) Shows that acetylcholine protected from esterase destruction by neostigmine can induce as much upregulation in 3 hours as can nicotine. Cells on 24 well plates were treated for 3 hrs with 300μM acetylcholine, 1 μM nicotine and 10μM neostigmine. After incubation the cells were washed 3 times with DMEM and fixed with 2% formaldehyde for 1 hour before labeling with

[^{3}H]epibatidine. Bound radioactivity was eluted by 200µl 0.1M NaOH. Protein concentration was calculated on wells in parallel experiment. B) Shows that quaternary amines slowly enter the ER and Golgi apparatus where they can compete for binding of [^{3}H]nicotine. The tertiary amines nicotine and epibatidine cross cell membranes very quickly to compete for binding within the cell. Cells on 96 wells plates were upregulated overnight with 0.5 µM nicotine to neutralize the effect of ongoing upregulation during incubation with quaternary amines. Then cells were washed three times with 200 µl DMEM. The drugs were added either 105 or 30 minutes before [^{3}H]nicotine or together with 5nM [^{3}H]nicotine, then incubated for an additional 20 min at 37^{0}C and 5% CO_2 before washing the cells with DMEM. The cells were washed 3 times with 200 µl DMEM, then bound radioactivity was eluted by 0.1M NaOH.

Fig. 10. Nicotine-induced upregulation of intracellular and surface AChRs. In (A) the time course of nicotine-induced upregulation is plotted. There is a rapid increase in intracellular α4β2 AChRs, followed after a lag of 3 hours by an increase in AChRs on the surface membrane. The mutant line starts with a somewhat higher level of total expression (2.1 pmol/mg protein) than wild type (0.9 pmol/mg), which could reflect either results of independent transfection and selection for the two lines or some intrinsic difference in expression of the two AChRs. After incubation in 0.5 µM nicotine for the indicated times, all 35 mm dishes of cells were simultaneously labeled with the membrane-impermeable reagent sulfo-NHS-LC biotin. Triton X-100 extracts from each plate were incubated with [^{3}H]epibatidine in wells coated with mAb 295 to β2 subunits to bind all AChRs or coated with streptavidin to bind surface labeled AChRs.

In (B) the same data as in (A) for the wild type cell line are presented as the ratio of surface to total AChRs. In (C) competitive inhibition of [^{3}H]epibatidine binding to surface AChRs by carbamylcholine was used to determine the proportion of surface and intracellular AChRs before and after upregulation. Binding to living cells attached to 35 mm plates was done in DMEM at 4^{o}C for only 15 min with 0.5 nM [^{3}H]epibatidine to minimize ongoing upregulation and penetration of quaternary amines inside the cells. To determine the internal pool of epibatidine binding sites, 10 mM of the quaternary amine carbamylcholine was added together with 0.5 nM [^{3}H]epibatidine to inhibit binding to cell surface AChRs. In (D) the proportion of the cell surface and intracellular AChRs before and after upregulation was measured by binding of [^{125}I] mAb 295 plus or minus permeabilization. Cells expressing $\alpha4\beta2$ AChRs were labeled with 2 nM [^{125}I] mAb 295 to $\beta2$ subunits after fixation for 1 hour using 2% phosphate buffered formaldehyde plus or minus permeabilization with 0.1% Triton X-100 for 1hour at room temperature. Incubation with 0.5 μM nicotine overnight increased binding of [^{125}I] mAb 295 to permeabilized cells only by 25%. Binding to the surface of cells that were not permeabilized with Triton X-100 was increased by 300%. Because this mAb binds only to $\beta2$ in association with $\alpha4$ (Ren et al., 2005), these results suggest much of the $\beta2$ in the cells is associated with $\alpha4$.

Fig. 11. Large pools of $\alpha4$ and $\beta2$ subunits in the cell line are demonstrated by western blots of Triton X-100 extracts of control and biotinylated cells. These are seen in crude extracts “C” at similar levels before and after upregulation overnight with 0.5 μM nicotine. Prior to upregulation, most subunits are in the unbound “U” fraction after adsorption with mAb 295 or

streptavidin bound to agarose, indicating that there are few mature pentameric AChRs and that any partially assembled α4 and β2 subunits are disrupted by Triton X-100 so that they can no longer bind to mAb 295. In fractions eluted with SDS from these adsorbents "E", initially only a small amount of assembled AChRs are present, but the amount increases greatly after upregulation. α4 and β2 subunits can be found at more than one molecular weight. This reflects differences in glycosylation. Removal of glycosylation using PNGase F resulted in single bands of lower molecular weights (data not shown). The effects of endoglycosidases which we observed were very similar to those of Sallette et al., (2005). The surface AChRs, which have been biotinylated and adsorbed by streptavidin indicate the glycosylation state of the mature surface AChRs.

Fig. 12. Sucrose gradient velocity sedimentation of Triton X-100 extracts from the α4β2 cell line shows a large increase in 10 S mature α4β2 AChRs after upregulation overnight with 0.5 μM nicotine. A) Shows binding of [^{3}H]epibatidine to AChRs immunoisolated from fractions of the gradient. Arrows indicate the position of *Torpedo* AChR 9.5 S monomers and 13 S dimers run as internal standards on the gradients. B) Shows western blots of α4 subunits in fractions from the gradient. β2 subunits were similarly distributed (data not shown). Samples were sedimented 16 hours at 40,000 rpm in an SW41 rotor on 5-20% sucrose gradients containing 0.5% Triton X-100. α4β2 AChRs were isolated for labeling with [^{3}H]epibatidine on wells coated with mAb 295. The *Torpedo* AChRs were isolated for labeling with [^{125}I] αBgt on microwells coated with mAb 210.

Fig. 13. DSP crosslinking of the α4β2 cell line reveals an 8.5 S component which can bind epibatidine and may be an assembly intermediate, easily dissociated by Triton X-100, to which nicotine binds to promote assembly of AChR pentamers. Cells were crosslinked for 2 hours on ice with 1 mM DSP in PBS before the reaction was stopped by adding 10 mM Tris pH 7.5 for 15 minutes, then rinsing 3 times with PBS. Sucrose gradient sedimentation was as in Fig. 11. Overnight upregulation with 0.5 μM nicotine increased the number of epibatidine labeled AChRs 13 fold in Triton extract fractions isolated on mAb 295 coated microwells, as shown in the left panel. The middle panel shows that DSP crosslinking before solubilization in Triton X-100 revealed the existence of an 8.5 S peak of partially assembled AChRs, which is usually dissociated by the detergent. The right panel shows the control samples of the middle and left panels. In the right panel 100% is defined for each of the gradients as the integrated number of binding sites on that gradient. This allows seeing the small control peaks, which are otherwise obscured by the large increase in the amount of AChR in the nicotine-treated samples in the left and middle panels.

Fig. 14. Nicotine treatment increases the half-life of surface membrane α4β2 AChRs. Nicotine treated cells were incubated for 16 hours with 0.5 μM nicotine. Prior to biotinylation the cells were detached with ice cold PBS and 5 mM EDTA, then washed twice by centrifugation with PBS only. The cells were surface labeled with Sulfo-NHS-LC biotin as in Fig. 10, then replated and grown with 0.5 μM nicotine for nicotine treated cells and without it for control cells. At the

Molecular Pharmacology Fast Forward. Published on September 23, 2005 as DOI: 10.1124/mol.105.012419
This article has not been copyedited and formatted. The final version may differ from this version.

indicated times, Triton X-100 extracts of cells were applied to streptavidin beads to isolate AChRs biotinylated on the cell surface. AChRs were quantitated by labeling with [^{3}H]epibatidine. The data represent the average of three experiments.

Molecular Pharmacology Fast Forward. Published on September 23, 2005 as DOI: 10.1124/mol.105.012419
This article has not been copyedited and formatted. The final version may differ from this version.

TABLES

Table 1.

Activation and Inhibition of α4β2 AChRs in a HEK Cell Line

	Receptors	Nicotine	Acetylcholine	DMPP	Cytisine	MCC	DHβE	Mecamyl-amine
Control								
Inhibition IC_{50} (nM)	α4β2	6.1±3.6					88±24	770±220
Activation EC_{50} (nM)	$(\alpha4)_2(\beta2)_3$	116±15	230±40	1,110±550	57±20	3,200±1,000	>1,000,000	
	$(\alpha4)_3(\beta2)_2$	2,700±200	57,000±20,000					
Nicotine Treated								
Activation EC_{50} (nM)	$(\alpha4)_2(\beta2)_3$	345±40	320±10	1,320±190			>1,000,000	
	$(\alpha4)_3(\beta2)_2$		71,000±37,000					

Molecular Pharmacology Fast Forward. Published on September 23, 2005 as DOI: 10.1124/mol.105.012419
This article has not been copyedited and formatted. The final version may differ from this version.

Table 2.

Upregulation of α4β2 AChRs in HEK Cell Lines

Values are mean ± S.E.M. Values reported in this table reflect binding of [^{3}H]epibatidine to fixed cells after 16 hours of upregulation. $C_{>95}$ is the concentration of drug required to achieve more than 95% of maximum upregulation.

Upregulation	**Line**	**Ligand Used to Induce Upregulation**						
		Nicotine	**Epibat-idine**	**DMPP**	**Cytisine**	**MCC**	**DHβE**	**Galant-amine**
Maximum Extent (upregulated/ control)	WT α4β2	4.9±0.9	5.4±1.4	5.5±1.1	5.2±1.3	5.8±1.9	3.3±0.6	2.2±0.2
	S247Fα4β2	2.9±0.5		2.5±0.9	2.5±0.5	2.4±0.7	1.3±0.2	2.2±0.2
Sensitivity EC_{50} nM $C_{>95}$, nM	WT α4β2	35±8 500	3.6±0.2 50	3800±1300 50,000	7.5±2.7 100	1500±500 50,000	3200±1600 500,000	3200±900 100,000
	S247Fα4β2	27±4 500		1700±700 20,000	5.8±2.1 100	7900±1300 100,000	5700±900 200,000	8400±2900 500,000

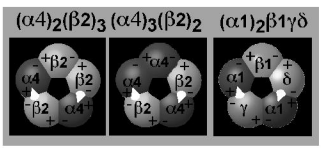

Figure 1

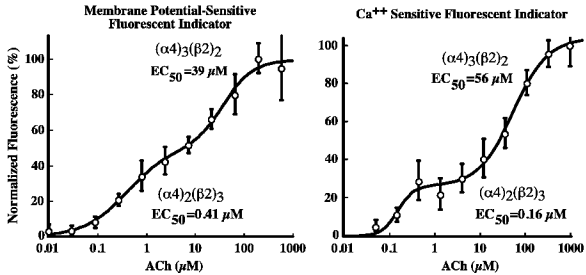
Membrane Potential-Sensitive Fluorescent Indicator
Normalized Fluorescence (%)
(α4)3(β2)2
EC50=39 μM
(α4)2(β2)3
EC50=0.41 μM
ACh (μM)
Ca++ Sensitive Fluorescent Indicator
(α4)3(β2)2
EC50=56 μM
(α4)2(β2)3
EC50=0.16 μM
ACh (μM)

Figure 2

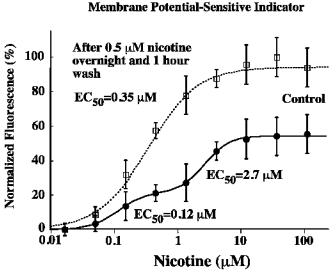
Membrane Potential-Sensitive Indicator
After 0.5 μM nicotine overnight and 1 hour wash
EC50=0.35 μM
Control
EC50=2.7 μM
EC50=0.12 μM
Normalized Fluorescence (%)
Nicotine (μM)
0
20
40
60
80
100
0.01
0.1
1
10
100

Figure 3

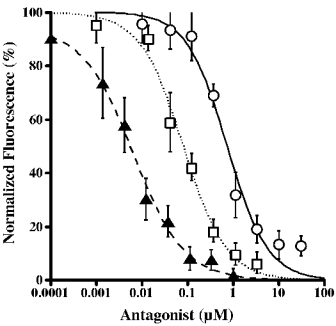
Normalized Fluorescence (%)
100
80
60
40
20
0
0.0001
0.001
0.01
0.1
1
10
100
Antagonist (μM)

Figure 4

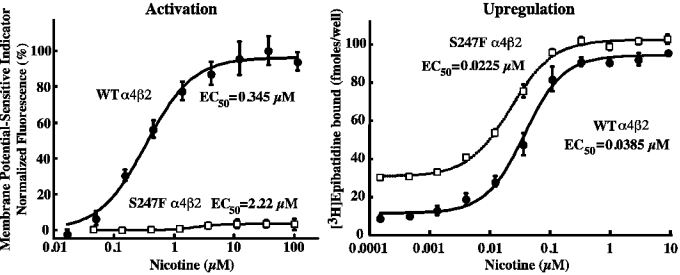
Activation
Membrane Potential-Sensitive Indicator
Normalized Fluorescence (%)
WT α4β2
EC50=0.345 μM
S247F α4β2 EC50=2.22 μM
Nicotine (μM)
Upregulation
[3H]Epibatidine bound (fmoles/well)
S247F α4β2
EC50=0.0225 μM
WT α4β2
EC50=0.0385 μM
Nicotine (μM)

Figure 5

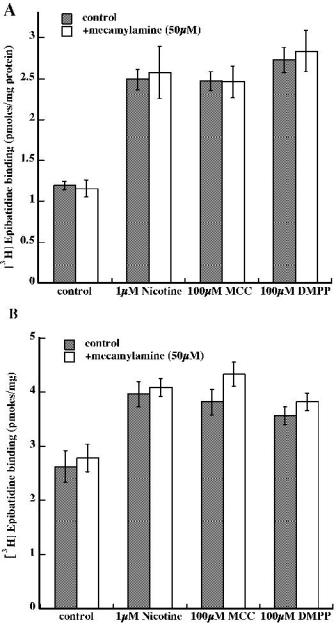
A
control
+mecamylamine (50μM)
[3H] Epibatidine binding (pmoles/mg protein)
0
0.5
1
1.5
2
2.5
3
control
1μM Nicotine
100μM MCC
100μM DMPP
B
control
+mecamylamine (50μM)
[3H] Epibatidine binding (pmoles/mg)
0
1
2
3
4
5
control
1μM Nicotine
100μM MCC
100μM DMPP

Figure 6

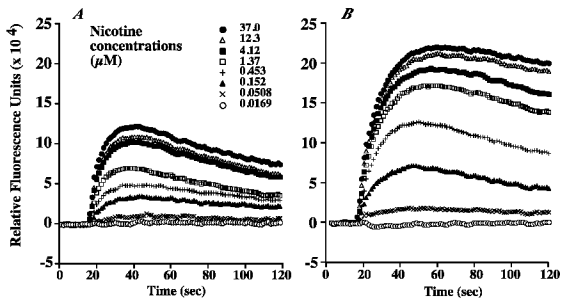
A
B
Nicotine concentrations (μM)
37.0
12.3
4.12
1.37
0.453
0.152
0.0508
0.0169
Relative Fluorescence Units (x 10 4)
Time (sec)
Time (sec)
25
20
15
10
5
0
-5
0
20
40
60
80
100
120

Figure 7

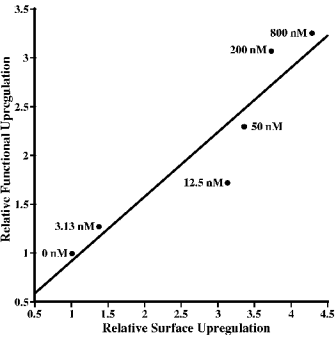
Relative Functional Upregulation
Relative Surface Upregulation
3.5
3
2.5
2
1.5
1
0.5
0.5
1
1.5
2
2.5
3
3.5
4
4.5
800 nM
200 nM
50 nM
12.5 nM
3.13 nM
0 nM

Figure 8

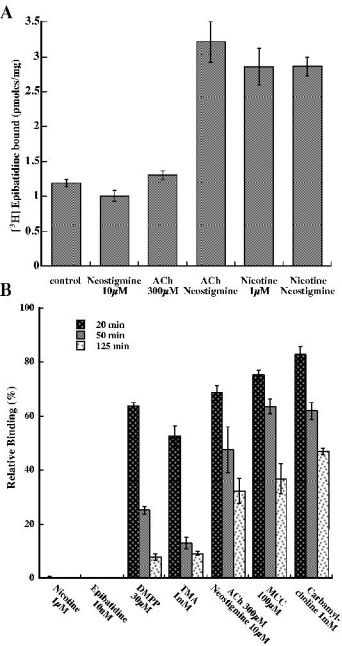
A
[3H] Epibatidine bound (pmoles/mg)
3.5
3
2.5
2
1.5
1
0.5
0
control
Neostigmine 10μM
ACh 300μM
ACh Neostigmine
Nicotine 1μM
Nicotine Neostigmine
B
Relative Binding (%)
100
80
60
40
20
0
20 min
50 min
125 min
Nicotine 1μM
Epibatidine 10nM
DMPP 300μM
TMA 1mM
ACh 300μM Neostigmine 300nM
MCC 100μM
Carbamylcholine 1mM

Figure 9

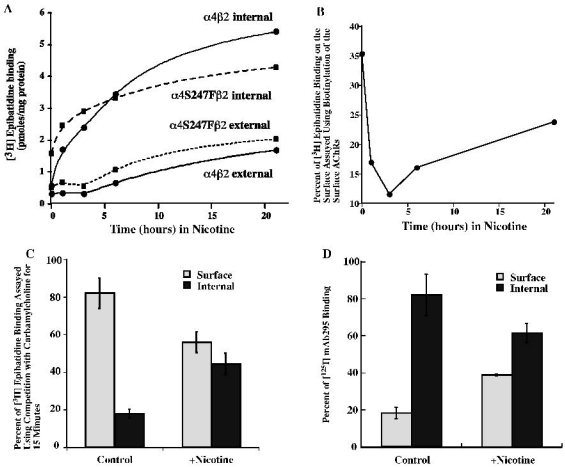
A
α4β2 internal
α4S247Fβ2 internal
α4S247Fβ2 external
α4β2 external
[3H] Epibatidine binding (pmoles/mg protein)
Time (hours) in Nicotine
B
Percent of [3H] Epibatidine Binding on the Surface Assayed Using Dissociation of the Surface AChRs
Time (hours) in Nicotine
C
Surface
Internal
Percent of [3H] Epibatidine Binding Assayed Using Competition with Carbamylcholine for 15 Minutes
Control
+Nicotine
D
Surface
Internal
Percent of [125I] mAb295 Binding
Control
+Nicotine

Figure 10

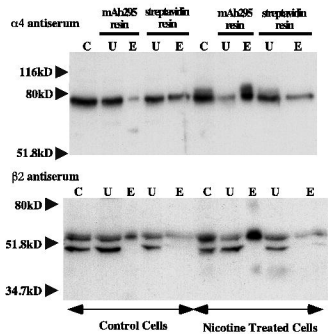
α4 antiserum
mAb295 resin
streptavidin resin
mAb295 resin
streptavidin resin
C U E U E C U E U E
116kD
80kD
51.8kD
β2 antiserum
C U E U E C U E U E
80kD
51.8kD
34.7kD
Control Cells
Nicotine Treated Cells

Figure 11

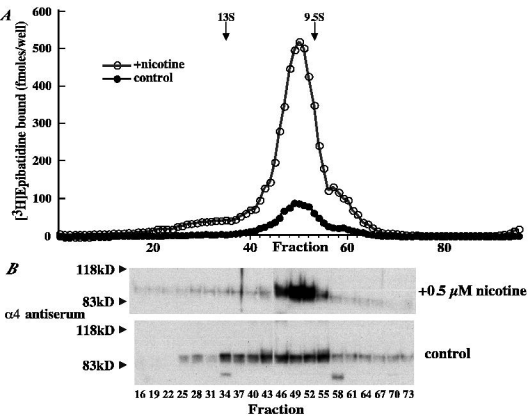
A
600
500
400
300
200
100
0
[3H]Epibatidine bound (fmoles/well)
13S
9.5S
+nicotine
control
20
40
Fraction
60
80
B
118kD
83kD
α4 antiserum
+0.5 μM nicotine
118kD
83kD
control
16 19 22 25 28 31 34 37 40 43 46 49 52 55 58 61 64 67 70 73
Fraction

Figure 12

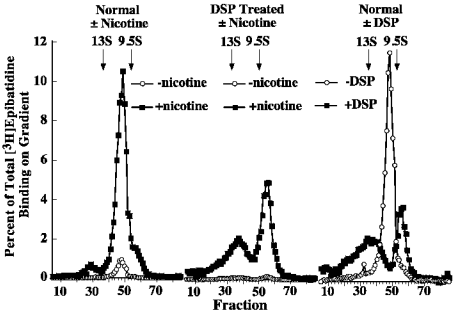
Normal
± Nicotine
13S 9.5S
DSP Treated
± Nicotine
13S 9.5S
Normal
± DSP
13S 9.5S
-nicotine
+nicotine
-nicotine
+nicotine
-DSP
+DSP
Percent of Total [3H]Epibatidine Binding on Gradient
0
2
4
6
8
10
12
10 30 50 70 10 30 50 70 10 30 50 70
Fraction

Figure 13

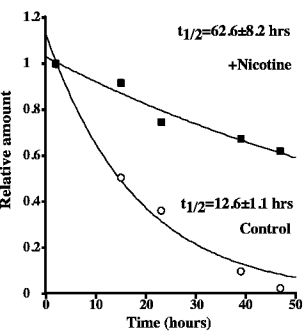
1.2
1
0.8
0.6
0.4
0.2
0
Relative amount
0
10
20
30
40
50
Time (hours)
t1/2=62.6±8.2 hrs
+Nicotine
t1/2=12.6±1.1 hrs
Control

Figure 14